Asian Journal of Mathematics and Computer Research

19(2): 75-86, 2017
ISSN: 2395-4205 (P), ISSN: 2395-4213 (O)

A NUMERICAL STUDY OF TURBULENT NATURAL CONVECTION IN A RECTANGULAR ENCLOSURE USING A TWO-EQUATION TURBULENCE MODEL

TIMOTHY KITUNGU NZOMO[1*] AND KENNEDY OTIENO AWUOR[1]
[1]School of Pure and Applied Sciences, Kenyatta University, Box 43844-00100, Nairobi, Kenya.

AUTHORS' CONTRIBUTIONS
This work was carried out in collaboration between both authors. Author TKN gathered the initial data, designed the study, obtained and interpreted the results. Author KOA read and approved the final manuscript.

Received: 24th December 2016
Accepted: 12th January 2017
Published: 5th August 2017

Original Research Article

ABSTRACT

Turbulent natural convection has been studied both numerically and theoretically. This work numerically studies turbulent natural convection in a rectangular enclosure with varying aspect ratios of 0.5, 1 and 2. The vertical walls of the enclosure are kept at a constant temperature difference of 10K while the horizontal walls are adiabatic. The work was carried for air as the fluid having a Prandtl number of 0.71. As the aspect ratio changed, the Rayleigh number changed from 10^8 to 10^{10}, due to the changing length of the enclosure. The finite volume based solver Fluent with Boussinesq approximation was used to conduct the numerical study. The k-omega two equation Reynolds Averaged Navier-Stoke Equations - based turbulence model was used for turbulent simulation. The velocity contours, streamlines and isotherms for the different Rayleigh numbers are studied. The results obtained show that as the aspect ratio increases, eddies at the top of the hot wall and at the bottom of the cold wall increase and the flow on the two vertical walls tend to exert more force on the stratified core. With the increasing Rayleigh number it is evident that the flow becomes characterized by a thin boundary layer adjacent to the vertical walls and a virtually stagnant thermally stratified core.

Keywords: Turbulent natural convection; heat transfer; rectangular enclosure; aspect ratio.

NOMENCLATURES

A_r : *Aspect ratio*
c_p : *Specific heat capacity, J/kgK*
e : *Specific internal energy, J/kg*
F_i : *External body force per unit volume in the i^{th} direction, N*
g : *Gravitational acceleration, m/s^2*
H : *Height of the enclosure, m*
k : *Turbulence kinetic energy, m^2/s^2*
K : *Thermal Conductivity of the fluid, $Wm^{-1}K^{-1}$*
L : *Length of the enclosure, m*

**Corresponding author: Email: nzomotimothy@gmail.com;*

M : *Mass flow, kg/s*
P : *Thermodynamic Pressure, Pa*
P_r : *Prandtl number*
Q : *Heat flux density, W/m²*
Ra : *Rayleigh number*
T : *Thermodynamic temperature, K*
t : *Time, s*
u, u', U : *Instantaneous velocity component in x-direction, fluctuation velocity and mean velocity in x-direction respectively, m/s*
U_* : *Characteristic velocity, m/s*
v, v', V : *Instantaneous velocity component in y-direction, fluctuation velocity and mean velocity in y-direction respectively, m/s*
x, y : *Horizontal and vertical Cartesian coordinates, m*

GREEK SYMBOLS

α : *Thermal diffusivity, m²/s*
β : *Thermal expansion coefficient, 1/K*
ΔT : *Temperature difference between hot and cold walls, K*
v : *Kinematic viscosity of the fluid, m²/s*
μ : *Dynamic viscosity, Ns/m²*
τ : *Shear stress, N/m²*
ρ : *Density of the fluid, kg/m³*
Δt : *Time interval, s*
δ_{ij} : *Kronecker delta*
δ : *Central difference operator*
ξ : *Non-dimensional temperature difference*
θ : *Non-dimensional temperature*
λ : *Thermal conductivity, W/mK*
Θ : *Non-dimensional mean temperature*
Ω_{ij} : *Vorticity*
ψ : *Stream function, m³/s*
ϕ : *Dissipation function*
∂ : *Differential operator*
∇ : *Del operator*
∇^2 : *Laplacian operator*
ω : *Specific dissipation, 1/s*
η : *Factor used to determine the degree of stretching.*

SUBSCRIPTS

b : *Boundary value*
c : *Cold wall*
h : *Hot wall*
$i, j,$: *i^{th} and j^{th} mesh points along the x and y directions respectively.*
0 : *Reference state*

SUPERSCRIPTS

n : *Current time step value*
$n+1$: *New time step value*
$'$: *Fluctuating component*
- : *Mean value*

1 Introduction

Turbulent natural convection flows are present in several science areas which include solar and stellar structures, the earth's mantle, atmospheric turbulence, engineering, electronics, etc. Natural convection flows can be either laminar or turbulent depending on the nature of the fluid in consideration and the geometrical conditions of the configuration under consideration. While laminar flow is well defined, turbulent flow is characterized by fluctuations in the fluid properties. This makes the flow to be random, diffusive and dissipative leading to high transport momentum, energy and mass. Natural convection as mode of heat transfer is generated by density differences in the fluid occurring due to temperature gradients. The fluid surrounding the heat source receives heat, becomes less dense and rises. The surrounding cooler fluid then moves to replace it. This cooler fluid is heated and the process continues, forming a convective current. The driving force for natural convection is buoyancy, a result of differences in fluid density. The Rayleigh number is the main parameter in natural convection. At values above 10^8 the flow becomes turbulent and hence the fluid properties become dependent of time and space. This creates eddies. Many authors have tried to evaluate the influence of temperature difference and aspect ratio on the fluid thermal behaviour inside the enclosure. The methods of study have been either experimental or numerical [1,2,3,4,5]. However experimental studies are expensive and hence the numerical approach which is cheaper is widely used. In this study turbulent natural convection in a rectangular enclosure is considered. The vertical walls are isothermal while the horizontal walls are adiabatic. The hot wall is kept at 305K while the cold wall is kept at 295K creating a temperature difference of 10K between them. The fluid used is air having a Prandtl number of 0.71. The length of the enclosure is varied from 0.5 to 2 m to vary the aspect ratio from 0.5 to 2 hence considering a Rayleigh numbers of 10^8 to 10^{10}. The accurate prediction of stream function and the isothermal distribution in the enclosure provides engineers with a feasibility study in the design of buildings, location and design of fire alarms, thermal energy storage alarms and electronic cooling systems. This is the main motivation of this study. In this study a brief theory of turbulent natural convection is given and general equations governing turbulent natural convection are then presented. The equations were then averaged using Reynolds decomposition to get the mean values. Then the equations were modelled to obtain both the k and ω - equation and finally using a non-dimensional form presented in their general form. The numerical solutions of the equations are then presented. The main objective of this study is to present the velocity contours, streamlines and isotherms in the enclosure as a result of temperature difference and how the aspect ratio affects them.

2 Literature Review

Turbulent natural convection is an area that continues to receive a lot of research attention due to its wide applications in engineering. In the past detailed experimental and numerical studies have been done as researchers try to understand turbulent flows.

[1] indicated that the rate of heat transfer is higher for a large window than for a small window as the Rayleigh number increases.

[2] investigated experimentally steady state heat transfer by natural convection from an enclosed assembly of thin vertical cylinders at high Rayleigh numbers. In this study experimental results showed that the surface temperature distribution increases axially up to a certain length, then decreases due to mixing which increases the heat transfer.

[3] examined numerically the turbulent natural convection of air in an enclosed tall cavity with high speed aspect ratio. In this study two cases of differential temperature were considered between the lateral cavity plates corresponding respectively to the low and high Rayleigh numbers: $Ra = 8.6 \times 10^5$ and $Ra = 1.43 \times 10^6$. For the two cases the flow was characterized by a turbulent low Reynolds number.

[4] extended the studies on natural turbulent convection and found that the provided correlation equation for the total average Nusselt number for both square and rectangular enclosures had a maximum deviation of 7.7 % compared to the numerical results.

[5] did a numerical study of a turbulent, natural convection with a compressible Large-Eddy simulation. The results of this study are compared to an analogue experimental setup of [6]. The results of the investigated fluid properties in all 3-dimensional simulations approximated well the experimental results.

[7] recorded a good summary of the transition form laminar flow to turbulence.

[8] found that the averaged flow and turbulent statistics are in good agreement with previous direct numerical simulations.

[9] compared the results of simulation of natural turbulent convection in a square cavity having isothermal vertical and highly heat conducting horizontal walls with the experimental data obtained for this cavity at a Rayleigh number equal to 1.58×10^9. In this study there was satisfactory agreement of the measured values with those predicted by the k-ε turbulence model.

[10] investigated numerically a steady bouncy-driven flow of air in a partially open square 2D cavity. It was found that for low Rayleigh numbers the isothermal curves are smooth and follow a parabolic shape indicating the dominance of the heat source.

[11] did Direct Numerical Simulations in the turbulent natural convection flow between two vertical walls kept at constant but different temperatures. It was found that gravity vector imposes a strong descending motion on the particles and this produces the increase of the particle concentration near the wall and reduction of the deposition velocities in comparison with the results without the gravity force.

[12] did a study to assess the performance of three numerical models k-ε , k-ω and *SST* k-ω turbulence model in predicting heat transfer due to natural convection in an air filled cavity. In this study he found that the room is stratified into three regions: the cold upper region, a hot region in the area between the heater and window and a warm lower region.

[13] numerically investigated laminar and turbulent natural convection. They found that deviations tend to increase for transitional and fully turbulent flows and that the steady state flow pattern is axi-symmetric and characterized by a single convection cell.

[14] conducted turbulent natural convection scaling in a vertical channel. The study showed that the resulting heat equation obtained by evaluating the inner and outer mean temperature wall functions contains a non-negligible correction term for the present Ra range as noted by [15].

[16] presented a study on free convection in a porous square cavity. Two energy models were employed giving results that indicated that when the ratio of thermal conductivities equals unity, both models gave similar results.

3 Methodology

3.1 The governing equations

The fundamental universal laws of conservation: conservation of mass, conservation of momentum and conservation of energy, are used to derive the general equations that govern the motion of a viscous Newtonian fluid experiencing convectional heat and mass transfer. These equations are expressed by use of partial differential equations [17].

$$\frac{\partial \rho}{\partial t} + \frac{\partial}{\partial x_j}(\rho u_j) = 0 \tag{1}$$

$$\frac{\partial}{\partial t}\rho u_i + \frac{\partial}{\partial x_j}(\rho u_i u_j) = -\frac{\partial P}{\partial x_i} + \rho g_i + \frac{\partial}{\partial x_j}\left[\mu\left(\frac{\partial u_i}{\partial x_j} + \frac{\partial u_j}{\partial x_i}\right)\right] + \mu_s \delta_{ij}\frac{\partial u_k}{\partial x_k} \tag{2}$$

$$\frac{\partial}{\partial t}\rho C_p T + \frac{\partial}{\partial x_j}(\rho C_p u_j T) = \frac{\partial}{\partial x_j}\left(\lambda \frac{\partial T}{\partial x_j}\right) + \beta T\left(\frac{\partial p}{\partial t} + \frac{\partial u_j P}{\partial x_j}\right) + \tau_{ij}\frac{du_i}{dx_j} \tag{3}$$

The equations are then decomposed using Reynolds decomposition to obtain,

$$\frac{\partial \bar{\rho}}{\partial t} + \frac{\partial}{\partial x_j}\left(\bar{\rho}\bar{u_j} + \overline{\rho' u'_j}\right) = 0 \tag{4}$$

$$\frac{\partial}{\partial t}\left(\bar{\rho}\bar{u_\iota} + \overline{\rho' u'_\iota}\right) + \frac{\partial}{\partial x_j}\left(\bar{\rho}\bar{u_\iota}\bar{u_j} + \bar{u_\iota}\overline{\rho' u'_j}\right) = -\frac{\partial \bar{p}}{\partial x_j} + \bar{\rho}\mathrm{g}_i + \frac{\partial}{\partial x_j}\left(\mu\left(\frac{\partial \bar{u_\iota}}{\partial x_j} + \frac{\partial \bar{u_j}}{\partial x_i}\right) + \mu_s \delta_{ij}\frac{\partial \bar{u_k}}{\partial x_k}\right) - uj\rho' u' i - \rho u' iu' j - \rho' u' iu' j \tag{5}$$

$$\frac{\partial}{\partial t}\left(c_p\bar{\rho}\bar{T} + c_p\overline{\rho' T'}\right) + \frac{\partial}{\partial x_j}\left(c_p\overline{\rho u_j}\bar{T}\right) = \frac{\partial \bar{p}}{\partial t} + \frac{\partial \bar{p}}{\partial x_j} + \overline{u'_\iota \frac{\partial p'}{\partial x_j}} + \frac{\partial}{\partial x_j}\left(\lambda\frac{\partial \bar{T}}{\partial x_j} - c_p\overline{\rho u'_\iota T'} - c_p\overline{\rho' u_\iota T'}\right) + \overline{\tau_{\iota J}}\frac{\partial \bar{u_\iota}}{\partial x_j} + \overline{\tau'_{\iota J}\frac{\partial u'_\iota}{\partial x_j}} \tag{6}$$

The Modeled k and ω equation are

$$\frac{\partial}{\partial t}\rho k + \frac{\partial}{\partial x_j}\left(\rho U_j k\right) = \overline{u_j}\frac{\partial}{\partial x_j}\mu\left(\frac{\partial U_\iota}{\partial x_j} + \frac{\partial U_J}{\partial x_\iota}\right) - \frac{1}{2}\frac{\partial}{\partial x_j}\overline{\rho u_\iota u_\iota u_j} - \rho\overline{u_\iota u_j}\frac{\partial U_i}{\partial x_j} + \overline{\rho u_\iota}\mathrm{g}_i - \overline{u_j\frac{\partial p}{\partial x_j}} \tag{7}$$

$$\frac{\partial \omega}{\partial t} + U_i\frac{\partial w}{\partial x_i} = \frac{\partial}{\partial x_j}\left[\left(\mu + \frac{\mu_t}{\sigma_\omega}\right)\frac{\partial \omega}{\partial x_i}\right] + \left[\beta - \frac{k^2}{\sigma_\omega\sqrt{c_\mu}}\right]\frac{\omega}{k}P_k - \beta\omega^2 \tag{8}$$

Non-dimensionalization is performed based on the following set of general scaling variables.

$$X_j = X'_j L_R,\ U_j = U'_j U_*,\ P = P' P_R,\ K = K' U_*,\ \Theta = \frac{T - T_*}{\Delta T_*},\ V = V'\mu_R,\ \mu'_s = \mu'_s \mu_R$$

$$\rho = \rho'\rho_R,\ t = \frac{t' L_R}{U_*},\ \mu = \mu'\mu_R,\ C_p = C_p C_{pR},\ \lambda = \lambda'\lambda_R,\ \omega = \frac{\omega' {U_*}^2}{L_R} \tag{9}$$

And then the following non-dimensional numbers substituted to obtain the final equations in their general form as shown

Table 1. Non-dimensional numbers

Froude number	$Fr = \sqrt{\frac{{U^2}_*}{\mathrm{g}L_R}}$
Reynolds number	$Re = \frac{\rho U_* L}{\mu}$
Non-dimensional temperature difference	$\xi = \frac{\Delta T_*}{T_R}$
Euler number	$Eu = \frac{P_R}{\rho_R {U^2}_*}$
Rayleigh number	$Ra = \frac{\mathrm{g}{\rho^2}_R C_{pR}\beta\Delta T_* {L^3}_R}{\mu_R k}$
Grashof number	$Gr = \frac{Ra}{Pr}$
Eckert number	$Ec = \frac{{U^2}_*}{C_{PR}\Delta T_*}$
Prandtl number	$Pr = \frac{\mu_R C_{PR}}{\lambda_R}$

Where $U_* = \sqrt{g\beta\Delta T_* L_R}$ in the above scheme.

$$\frac{\partial \rho}{\partial t} = \frac{\partial}{\partial x_j}\left(\rho U_j + \overline{\rho u_j}\right) = 0 \tag{10}$$

$$\frac{\partial}{\partial t}(\rho U_i + \overline{\rho u_i}) + \frac{\partial}{\partial x_j}\left(\rho U_i U_j + U_i\overline{\rho u_j}\right) = -\left(\frac{Eu.Fr}{\xi\eta}\right)\frac{\partial P}{\partial x_i} + \left(\frac{1}{\xi\eta}\right)\rho g_i + \frac{\partial}{\partial x_j}\left[\frac{1}{\sqrt{Gr}}\tau_{ij} - U_j\overline{\rho u_i} - \rho\overline{u_i u_j} - \rho uiuj\right] \tag{11}$$

$$\frac{\partial}{\partial t}\left(C_p\rho\Theta + C_p\overline{\rho\theta}\right) + \frac{\partial}{\partial x_j}\left(C_p\rho U_j\Theta\right) = Eu.Ec\left[\frac{\partial P}{\partial t} + U_j\frac{\partial P}{\partial x_j} + u_j\frac{\partial P}{\partial x_j}\right] + \frac{\partial}{\partial x_j}\left[\frac{1}{Pr\sqrt{Gr}}\lambda\frac{\partial\Theta}{\partial x_j} - C_P\rho\overline{u_i\theta} - CpC_p\rho ui\theta Ec.Re - 1\phi\right] \tag{12}$$

$$\frac{\partial}{\partial t}\rho k + \frac{\partial}{\partial x_j}\rho U_j k = \frac{1}{\sqrt{Gr}}u_j\frac{\partial}{\partial x_j}\mu\left[\frac{\partial u_i}{\partial x_j} + \frac{\partial u_j}{\partial x_i}\right] - \frac{1}{2}\frac{\partial}{\partial x_j}\rho\overline{u_i u_i u_j} - \rho\overline{u_i u_j}\frac{\partial U_i}{\partial x_j} + \frac{1}{\xi\eta}\overline{\rho u_i}g_i - \frac{Eu.Fr}{\xi\eta}\overline{u_j\frac{\partial P}{\partial x_i}} \tag{13}$$

$$\frac{\partial}{\partial t}\rho\omega + \frac{\partial}{\partial x_j}\rho U_j\omega = -2\frac{1}{\sqrt{Gr}}\mu\overline{\frac{\partial u_i}{\partial x_j}} - 2\frac{1}{Gr}\rho\overline{\left(v\frac{\partial^2 u_i}{\partial x_k\partial x_j}\right)^2} + 2\frac{Fr}{\sqrt{Gr}}v\overline{\frac{\partial u_i}{\partial x_j}\frac{\partial\rho}{\partial x_j}}g_i - 2\frac{1}{\sqrt{Gr}}\mu\left[\overline{\frac{\partial u_i}{\partial x_j}} + \overline{\frac{\partial u_j}{\partial x_i}}\right] - 2\frac{1}{\sqrt{Gr}}\mu\frac{\partial^2 u_i}{\partial x^2{}_j}\overline{\frac{\partial u_i}{\partial x_j}} \tag{14}$$

3.2 Mathematical model

In this study, turbulent natural convection is studied numerically by solving the system in the scheme shown in Fig. 1 below. This is a two dimensional flow of an ideal gas in a rectangular enclosure of height H and length L. The two horizontal walls are adiabatic. The other two vertical walls in the x-direction are isothermal with the left wall being maintained at 305K and the right wall at 295K.

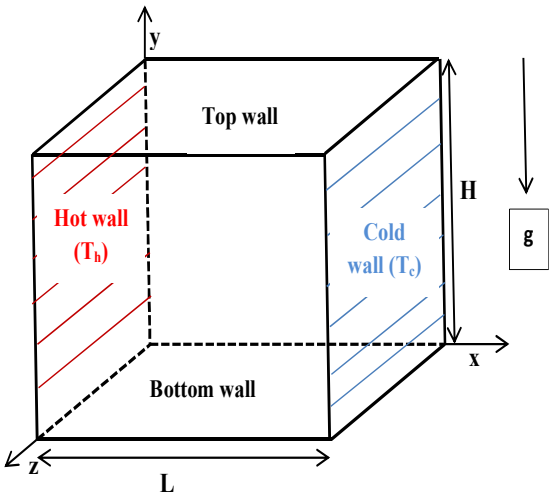

Parameters

T_h = 305K

T_c = 295K

Pr = 0.71

ρ = 1.1765 kg/m^3

C_p = 1006.3J/kgK

K = 0.026118W/mK

β = 3.3317 × 10^{-3} K^{-1}

g = 9.81m/s^2

Fig. 1. Schematic diagram of the rectangular enclosure

3.3 Boundary conditions

$\frac{\partial\Theta}{\partial n} = 0, \Theta_{hot} = 1, \Theta_{cold} = o, v = u = o, \psi = 0$ and $\frac{\partial\psi}{\partial n} = 0.$

In order to solve the equations derived we employ a numerical method. The finite difference method is employed in this study. To be in a position to replace the partial spatial and time derivatives with finite difference approximation, the system is solved using an explicit time evaluation. The spatial domain is discretized by two dual orthogonal regular Cartesian grids based on squares with spatial subdivisions of Δx and Δy, whereas the time domain is subdivided into intervals of Δt. Since we are using the vorticity-stream function formulation in this study, there is no need for a staggered finite difference grid system.

4 Results and Discussion

4.1 Velocity contours and streamlines

The results of this study are shown in Figs. 2 - 7 which illustrates the velocity contours in terms of the velocity magnitude and stream function and also the distribution of isotherms within the enclosure, stream function being the scalar function whose contour lines define the streamlines. The velocity contours of showing velocity magnitude shows a concentration of the vortices around the top left of the hot wall and around the bottom right of the cold wall. At constant temperature, as the aspect ratio is increased the vortices become bigger and become less as they disappear along the edges. Considering the velocity contours of stream function which shows the stream lines, the circulating vortices are concentrated around the top upper left of the hot wall and around the bottom right of the cold wall. As the aspect ratio increases at constant temperature the vortices around the two corners become small and some disappear. This shows that since the aspect ratio is being varied by varying the length of the enclosure, the Rayleigh number increases as the aspect ratio increases, increasing the buoyancy forces and hence leading to an increase in the strength of the stream function. It can be seen that the unsteady eddies observed at the top of the hot wall and at the bottom of the cold wall are increasing with an increase in aspect ratio and the flow on the two vertical walls is exerting more force on the stratified core. This core tends to shrink more with increase in the aspect ratio varying the stream lines from the horizontal till some disappear.

4.2 Isotherms

Looking at the temperature distribution in the enclosures, we consider the isotherms which are lines connecting points of equal temperature. They show us the variation of temperature over space. Figs. 8-10 shows the isothermal distribution in the enclosures as the aspect ratio is changed which in turn varies the Rayleigh number as indicated. The heat flows from the hotter wall towards the cold wall forming thermal boundary layers as the aspect ratio increases. The core again is seen to shrink as the aspect ratio increases and the isothermal lines vary from the horizontal until they disappear.

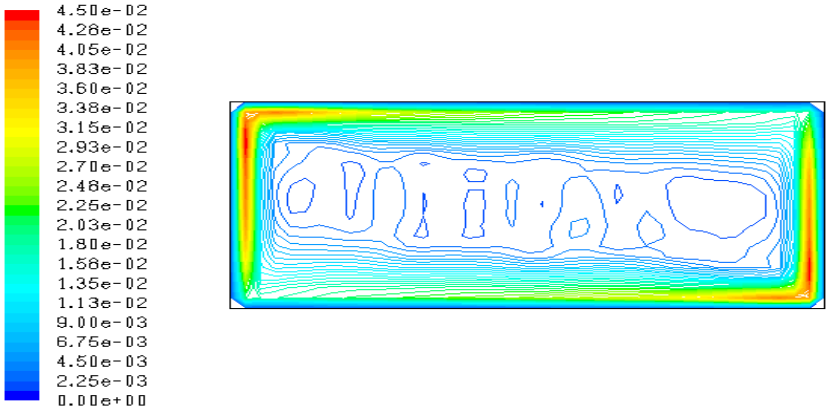

Fig. 2. Velocity contours for $A_r = 0.5$ (Ra = 1.5×10^{10})

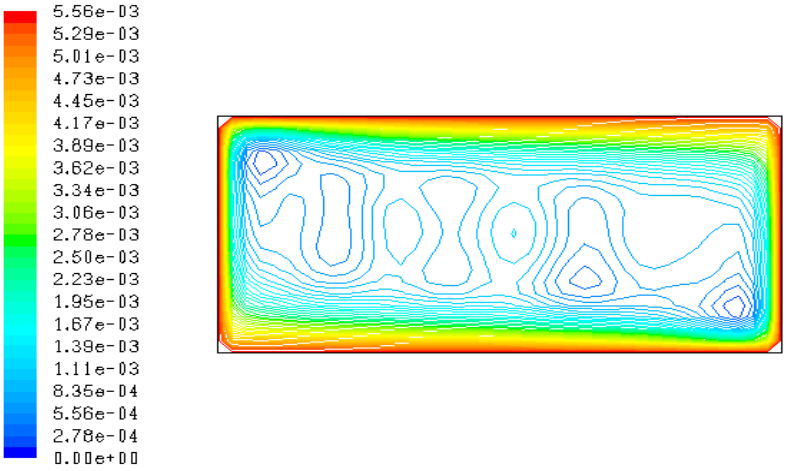

Fig. 3. Streamlines for $A_r = 0.5$ (Ra = 1.5×10^{10})

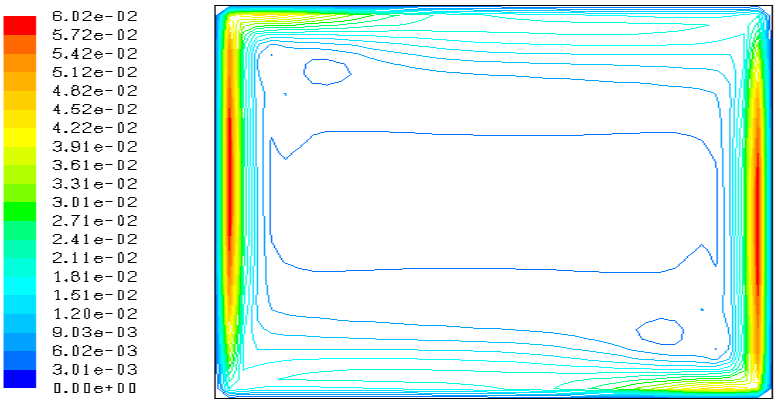

Fig. 4. Velocity contours for $A_r = 1$ (Ra = 1.9×10^{9})

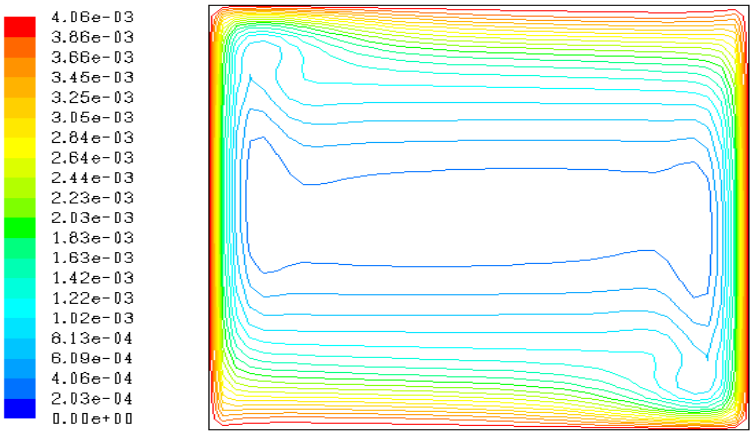

Fig. 5. Streamlines for $A_r = 1$ (Ra = 1.9×10^{9})

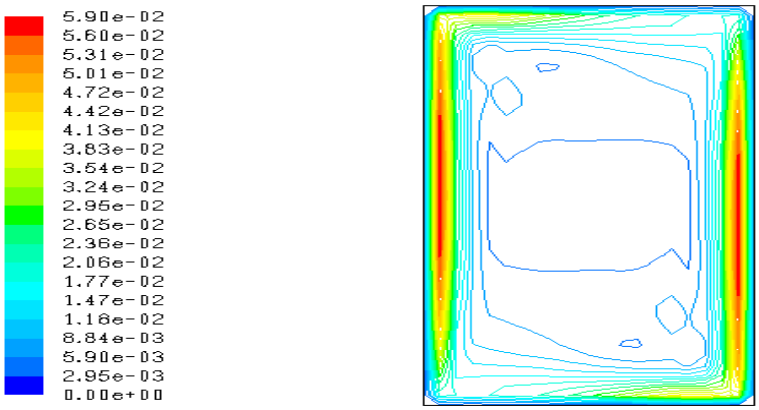

Fig. 6. Velocity contours for $A_r = 2$ (Ra = 2.3× 10^8)

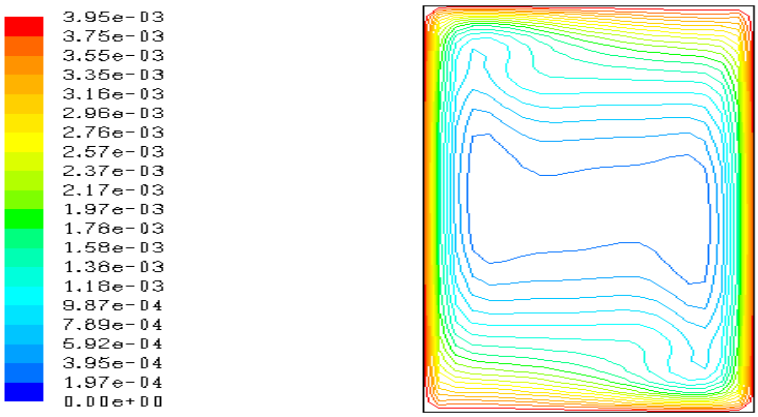

Fig. 7. Streamlines for $A_r = 2$ (Ra = 2.3× 10^8)

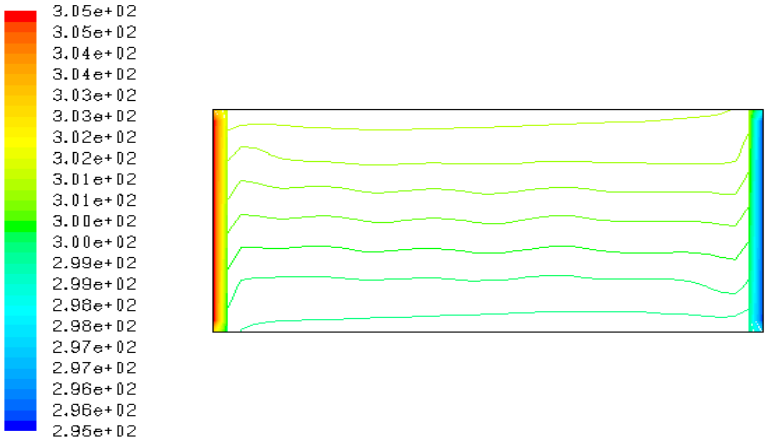

Fig. 8. Isotherms for $A_r = 0.5$ (Ra = 1.5× 10^{10})

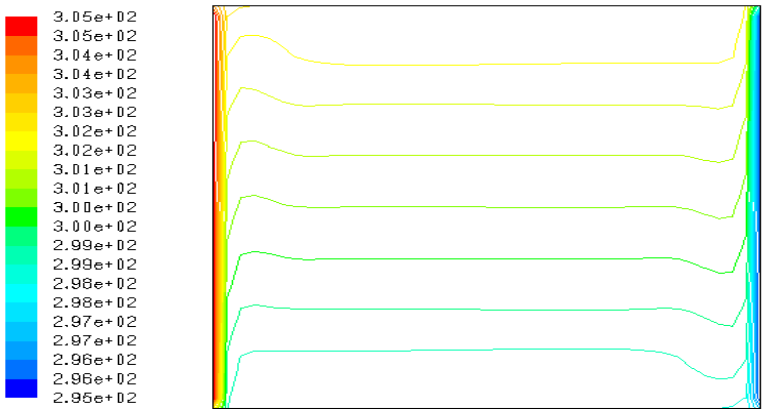

Fig. 9. Isotherms for $A_r = 1$ (Ra = 1.9× 10^9)

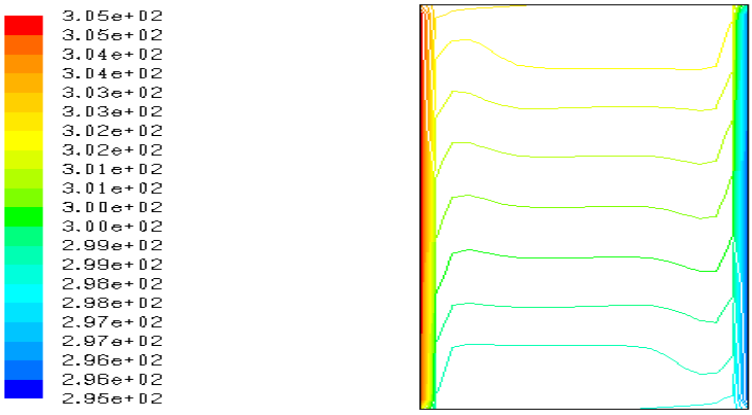

Fig. 10. Isotherms for $A_r = 2$ (Ra = 2.3× 10^8)

5 Conclusion

A numerical simulation of turbulent natural convection in an enclosure has been done. A rectangular enclosure filled with air of Prandtl number 0.71 was considered. The temperature between the two walls was kept constant at 10K and the aspect ratio varied by varying the length of the enclosure which in turn varied the Rayleigh number. The governing equations were derived. The equations were then averaged using Reynolds decomposition to get the mean values. Then the equations were modeled to obtain both the *k* and ω - equation and finally using a non-dimensional form presented in their general form. The finite volume based solver Fluent with Boussinesq approximation was used to conduct the numerical study using the k-omega two equation Reynolds averaged Navier-Stokes (turbulence based model). The equations were discretized using second order central difference approximation in space and the convective terms differentiated using the Alternating Direction Implicit (ADI) method. The results were presented in terms of the velocity magnitude and stream function as well as the isotherms. The results showed that as the length increased which in turn increased the Rayleigh number, the stream function became stronger and thus increasing the number of vortices. This decreases the thickness of the thermal boundary layer and hence concentrating the vertices at the upper parts of the enclosure. The results of this study showed good agreement with benchmark results of [18]. Thus this study provides engineers with good results for industrial, electrical and civil engineering applications.

6 Recommendations

In this numerical study, the aspect ratio was varied by varying the length of the enclosure while the temperature between the two vertical walls was kept constant. It is recommended that further study be carried out for:

a) A varying aspect ratio determined by changing the height of the enclosure.
b) A varying aspect ratio as a result of temperature change between the walls.

Competing Interests

Authors have declared that no competing interests exist.

References

[1] Gatheri FK, Reizes JA, Leonardi E, de Vahl Davis. Natural convection in an enclosure with colliding boundary layers, a numerical study. AHMT Conference Brisbane, Australia; 1993.

[2] Arshad M, Mansoor HI, Imran RC. Experimental study of natural convection heat transfer from an enclosed assembly of thin vertical cylinders. Applied Thermal Engineering. 2010;31:20-27.

[3] Mohamed A, Amina M, Nassim S, Zoubida H. Rayleigh number effect on the turbulent heat transfer within a parallelepiped cavity. Thermal Science. 2011;15(2):S341-S356.

[4] Shati AKA, Blakey SG, Beck SBM. An empirical solution to turbulent natural convection and radiation heat transfer in square and rectangular enclosures. Applied Thermal Engineering. 2013;51: 364-370.

[5] Zimmermann C, Groll R. Modeling turbulent heat transfer in a natural convection flow. Journal of Applied Mathematics and Physics. 2014;2:662-670.

[6] Ampofo F, Karayiannis TG. Experimental benchmark data for turbulent convection in an air-filled square cavity. International Journal of Heat and Mass Transfer. 2003;46:3551-3572.

[7] Yang KT. Transitions and bifurcations in laminar buoyant flows in confined enclosure. Journal of Heat Transfer. 1988;110:1191-1203.

[8] Pallares J, Vernet A, Ferre JA, Grau FX. Turbulent large-scale structures in natural convection vertical channel flow. International Journal of Heat and Mass Transfer. 2010;53:4168-4175.

[9] Fomichev AI. Comparison of the results of modeling convective heat transfer in turbulent flows with experimental data. Journal of Engineering Physics and Thermophysics. 2010;83:5.

[10] Eliton F, Adriano S, Viviana CM. Natural convection in partially open square cavity with internal heat source: An analysis of opening mass flow. International Journal of Heat and Mass Transfer. 2011;54:1369-1386.

[11] Pallares J, Grau FX. Particle dispersion in a turbulent natural convection channel flow. Journal of Aerosol Science. 2012;43:45-56.

[12] Awuor KO. Simulating natural turbulent convection fluid flow in an enclosure using the two-equation turbulent models, a PhD thesis. Kenyatta University, Kenya; 2012.

[13] Feldman Y, Colonius T. On a transitional and turbulent natural convection in spherical shells. International Journal of Heat and Mass Transfer. 2013;64:514-525.

[14] Ng CS, Chung D, Ooi A. Turbulent natural convection scaling in a vertical channel. International Journal of Heat and Fluid Flow. 2013;44:554-562.

[15] George WK, Capp SP. A theory for natural convection turbulent boundary layers next to heated vertical surfaces. International Journal of Heat and Mass Transfer. 1979;22:813-826.

[16] Paolo HS, Marcelo JS. Turbulent free convection in a porous cavity using the two-temperature model and the high Reynolds closure. International Journal of Heat and Mass Transfer. 2014;79:105-115.

[17] Currie IG. Fundamental of fluids. McGraw-Hill Inc.; 1974.

[18] Markatos NC, Periceuos KA. Laminar and turbulent natural convection in an enclosed cavity. International Journal Heat and Mass Transfer. 1984;27(5):755-772.